Local staging of prostate cancer with MRI

Fatma Nur Soylu, Scott Eggener, Aytekin Oto

ABSTRACT
Accurate local staging of prostate cancer is essential for patient management decisions. Conventional and evolving magnetic resonance imaging (MRI) techniques, such as diffusion-weighted imaging, dynamic contrast-enhanced MRI, and MR spectroscopy, are promising techniques in prostate cancer imaging. In this article, we will review the current applications of conventional and advanced MRI techniques in the local staging of prostate cancer.

Key words: • prostate cancer • tumor staging • magnetic resonance imaging

Accurate local staging of prostate cancer is critical for patient management decisions. The presence of locally advanced prostate cancer, in the form of extracapsular extension, seminal vesicle invasion, or regional lymph node metastasis, can affect the choice of treatment. In the last decade, magnetic resonance imaging (MRI) of the prostate has evolved and improved with the introduction of advanced MRI techniques, such as diffusion-weighted imaging (DWI), dynamic contrast-enhanced MRI (DCE MRI), MR spectroscopy (MRS), and new technologies such as 3 Tesla (T) MRI and endorectal coils. Recently, conventional and advanced MRI have been adopted for prostate cancer imaging and appear to be promising imaging techniques for use in the local staging of this disease. In this article, we will review the current use of these MRI techniques in the local staging of prostate cancer.

Staging of prostate cancer

Although there are several different staging systems for prostate cancer, the most widely used system is currently the TNM system. In the TNM staging system, T1 refers to organ-confined tumors that are clinically and radiologically occult. T2 refers to organ-confined tumors that are clinically or radiologically apparent. T3 refers to tumors that extend outside the prostatic capsule in the form of extracapsular extension or seminal vesicle invasion. T4 refers to tumors that invade adjacent structures. N1 indicates the presence of locoregional lymph node metastasis, and M1 indicates the presence of distant metastases. The American Joint Committee on Cancer has incorporated prognostic information from the Gleason score and preoperative prostate-specific antigen (PSA) levels into the TNM system (1).

The most crucial aspect of prostate cancer staging is differentiating between organ-confined and non-organ-confined disease. Extracapsular extension is associated with a greater risk of a positive surgical margin, further decreasing the chance of long-term cancer control (2, 3). Seminal vesicle invasion is associated with an increased incidence of lymph node metastasis and a worse prognosis (4). The presence of lymph node metastasis at the time of prostate cancer diagnosis is associated with a high probability of progression to distant metastases and a poor prognosis (5, 6). The probability of the presence of extracapsular extension, seminal vesicle invasion, and lymph node metastasis is determined clinically from staging nomograms, such as the Kattan and Partin nomograms, which estimate the pathologic stage based on the pretreatment PSA level, the clinical stage, and the Gleason grade of the biopsy specimen (7, 8). Although it has been reported that staging nomograms do not incorporate the results of imaging studies that could assist in predicting extracapsular extension and seminal vesicle invasion (3, 8, 9), MRI contributes significant incremental value to the nomograms for the

From the Department of Radiology (F.N.S. ✉ nursoylu@yahoo.com, A.O.) and the Department of Surgery, Section of Urology (S.E.), University of Chicago, Chicago, Illinois, USA.

prediction of extracapsular extension, seminal vesicle invasion, and lymph node metastasis. Additionally, intermediate and high-risk patients have been reported to derive the greatest benefit from MRI (10).

Staging with MRI

MRI is generally considered to be the most accurate imaging method for the local staging of prostate cancer (11). However, when used for prostate cancer staging, MRI has a wide range of accuracy, sensitivity, and specificity values. Differences in patient selection, study protocols, MR equipment, type of coil, reader experience in prostate MRI, and a lack of standard diagnostic criteria for staging may explain the wide range of these values (12). To investigate the differences between reports on the staging of prostate cancer, Engelbrecht et al. (12) conducted a meta-analysis of 146 studies, performed between January 1984 and May 2000. This study showed that MRI has a combined sensitivity and specificity of 71% in detecting extracapsular extension and seminal vesicle invasion. It also showed that the use of the spin echo sequence, an endorectal coil and multiple imaging planes improve staging performance (12). Compared with pelvic phased array coils alone, MRI with an endorectal surface coil provides higher resolution images with a superior prostatic and periprostatic signal-to-noise ratio (13, 14). Most prostate MRI examinations are performed using an air-filled endorectal coil that causes magnetic susceptibility gradients within the gland. Filling the endorectal coil with a perfluorocarbon (PFC) compound has been shown to improve the diagnostic quality of MRS (15). Inflating the endorectal coil with a barium suspension may be an alternative to inflation with PFC in prostate MR studies, especially at high field strengths (such as 3 T) (16).

Three Tesla scanners provide a better signal-to-noise ratio, allowing improved spatial and temporal resolution in prostate cancer imaging. Heijmink et al. (17) reported a significant improvement in image quality and staging performance with an endorectal coil compared to a body-array coil, using a 3 T MRI. A learning curve has also been described for local staging of prostate cancer, and MR staging performance improves with experience (11).

Recently, in a consensus meeting, 16 expert authors attempted to make recommendations regarding the standardization of multiparametric MRI for detecting, localizing, and characterizing prostate cancer. The agreement rate was relatively low (approximately 60%) for defining the criteria, which mainly concerned conducting, interpreting, and reporting MRIs in patients with prostate cancer (18). This shows that determining such criteria is extremely difficult. Nevertheless, similar studies are needed for prostate cancer staging.

T2-weighted MRI

Conventional T2-weighted sequences were the first MRI techniques to localize and stage prostate cancer and are still the most widely used imaging sequences. Prostate zonal anatomy and prostate cancer are best observed on multiplanar T2-weighted MRI. Furthermore, the prostatic capsule appears as a thin rim of low signal intensity surrounding the peripheral zone, and the seminal vesicles, which demonstrate high signal intensity because of their fluid content, are best evaluated anatomically on T2-weighted MRI. Lymphadenopathy can also be demonstrated easily by T2-weighted imaging. Hence, thin-section, high-spatial resolution fast spin-echo T2-weighted images in the axial, sagittal, and coronal planes are the main sequences for the local staging of prostate cancer with MRI.

Extracapsular extension with T2-weighted MRI

In previous studies, the reported sensitivities and specificities of MRI for the detection of extracapsular extension were in the range of 29%–80% and 47%–100%, respectively (19–23). Patients with a tumor volume larger than 0.3 cm^3 are at a high risk of developing extracapsular extension (24). Criteria for detecting extracapsular extension on T2-weighted MRI include at least one of the following: irregular capsular bulge, disruption of the prostatic capsule, extension into the periprostatic fat, broad contact with the capsule (>12 mm), obliteration of the rectoprostatic angle, or asymmetry or involvement of the neurovascular bundles (Figs. 1 and 2) (25, 26). Multivariate analysis has shown that obliteration of the rectoprostatic angle

and asymmetry of the neurovascular bundle are the strongest predictive factors for extracapsular extension (25). Tempany et al. (27) reported that the sensitivity, specificity, and overall accuracy of T2-weighted MRI for neurovascular bundle invasion were 68%, 59%, and 64%, respectively.

Seminal vesicle invasion with T2-weighted MRI

In previous studies, sensitivity and specificity levels for diagnosing seminal vesicle invasion with MRI were in the range of 22%–77% and 80%–99%, respectively (19–22, 28). The main diagnostic criteria for seminal vesicle invasion on T2-weighted MRI are the lack of normal seminal vesicle architecture, focal or diffuse areas of low signal intensity within the seminal vesicle, low signal intensity within the seminal vesicle causing mass effect, enlarged ejaculatory ducts with low signal intensity, thickening of the ductus deferens, obliteration of the angle between the prostate and seminal vesicle on sagittal images, direct extension of the low signal intensity of tumor from the base of the prostate to the seminal vesicle, and non-contiguous areas of low signal intensity within the seminal vesicle (20, 29). Low signal intensity within the seminal vesicle and lack of preservation of the normal architecture of the seminal vesicle have shown the highest sensitivity and specificity with T2-weighted MRI (Fig. 3) (20). The presence of hemorrhage after biopsy can also result in low signal intensity within the seminal vesicle. Therefore, it is critical to combine the pre-contrast T1-weighted images with T2-weighted images in the evaluation of seminal vesicle invasion. In hemorrhage, the lower signal intensity of the seminal vesicle wall and the architecture of the seminal vesicle are preserved (20). Additionally, inflammation, amyloidosis, atrophy, or inadequate distention of the seminal vesicles may cause wall thickening and complicate the evaluation for tumor invasion by prostate cancer.

Lymph node metastasis with T2-weighted MRI

In previous studies, MRI has been shown to have a low sensitivity (27%–60%) for the detection of lymph node metastasis, although it has a high specificity (98%) and negative
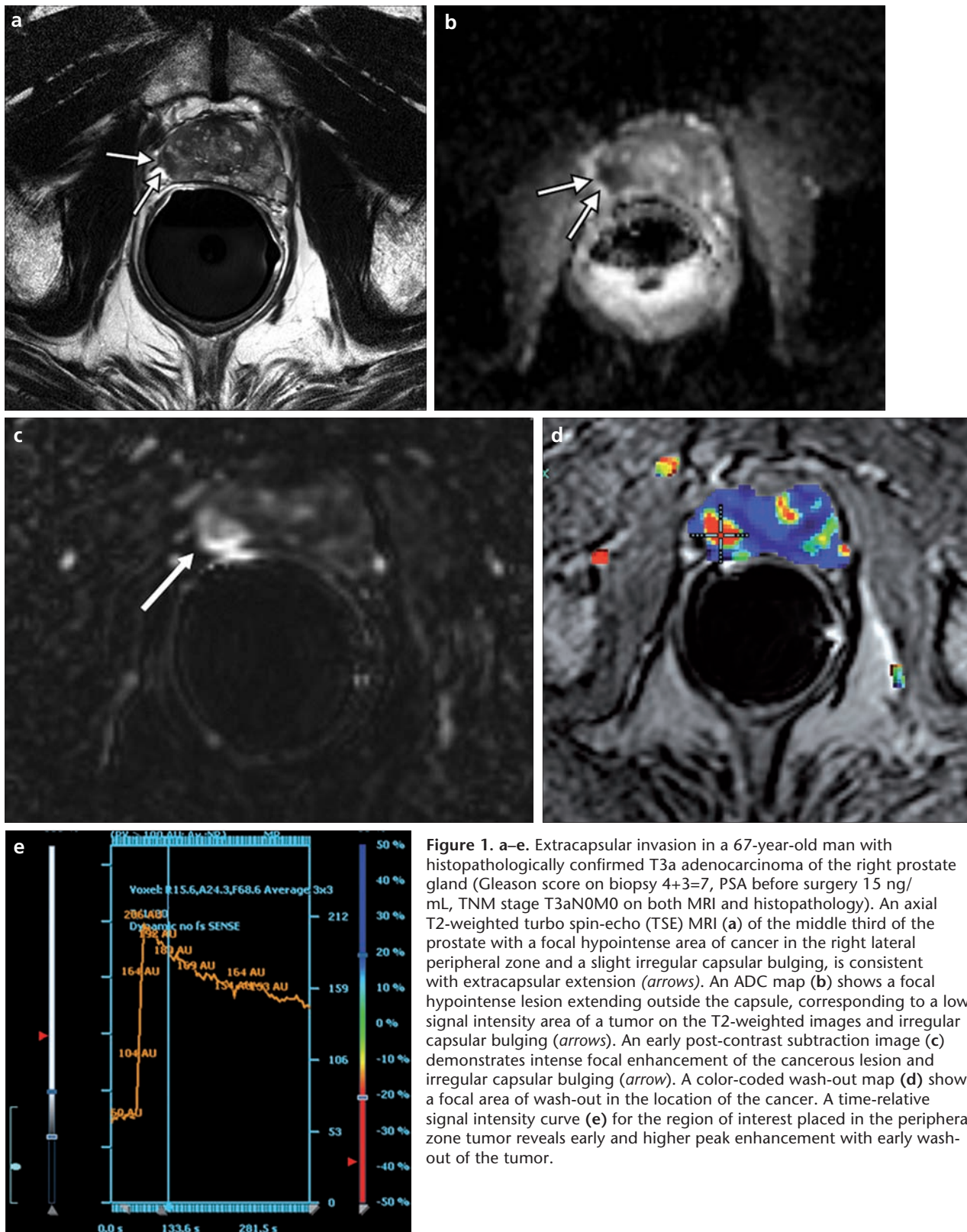
Figure 1. a–e. Extracapsular invasion in a 67-year-old man with histopathologically confirmed T3a adenocarcinoma of the right prostate gland (Gleason score on biopsy 4+3=7, PSA before surgery 15 ng/mL, TNM stage T3aN0M0 on both MRI and histopathology). An axial T2-weighted turbo spin-echo (TSE) MRI (**a**) of the middle third of the prostate with a focal hypointense area of cancer in the right lateral peripheral zone and a slight irregular capsular bulging, is consistent with extracapsular extension *(arrows)*. An ADC map (**b**) shows a focal hypointense lesion extending outside the capsule, corresponding to a low signal intensity area of a tumor on the T2-weighted images and irregular capsular bulging *(arrows)*. An early post-contrast subtraction image (**c**) demonstrates intense focal enhancement of the cancerous lesion and irregular capsular bulging *(arrow)*. A color-coded wash-out map (**d**) shows a focal area of wash-out in the location of the cancer. A time-relative signal intensity curve **(e)** for the region of interest placed in the peripheral zone tumor reveals early and higher peak enhancement with early wash-out of the tumor.

predictive value (96%) (30–32). With conventional MRI, the major criteria for lymph node metastasis assessment are the size and, to a lesser extent, the shape of the lymph node. Lymph nodes are considered to be malignant if the short axis diameter is elongated and larger than 10 mm in diameter or is round and larger than 8 mm in diameter (Fig. 4) (31).

Diffusion-weighted MRI

DWI is based on the movement of water molecules within the intracellular and extracellular spaces. This movement causes a signal decay on
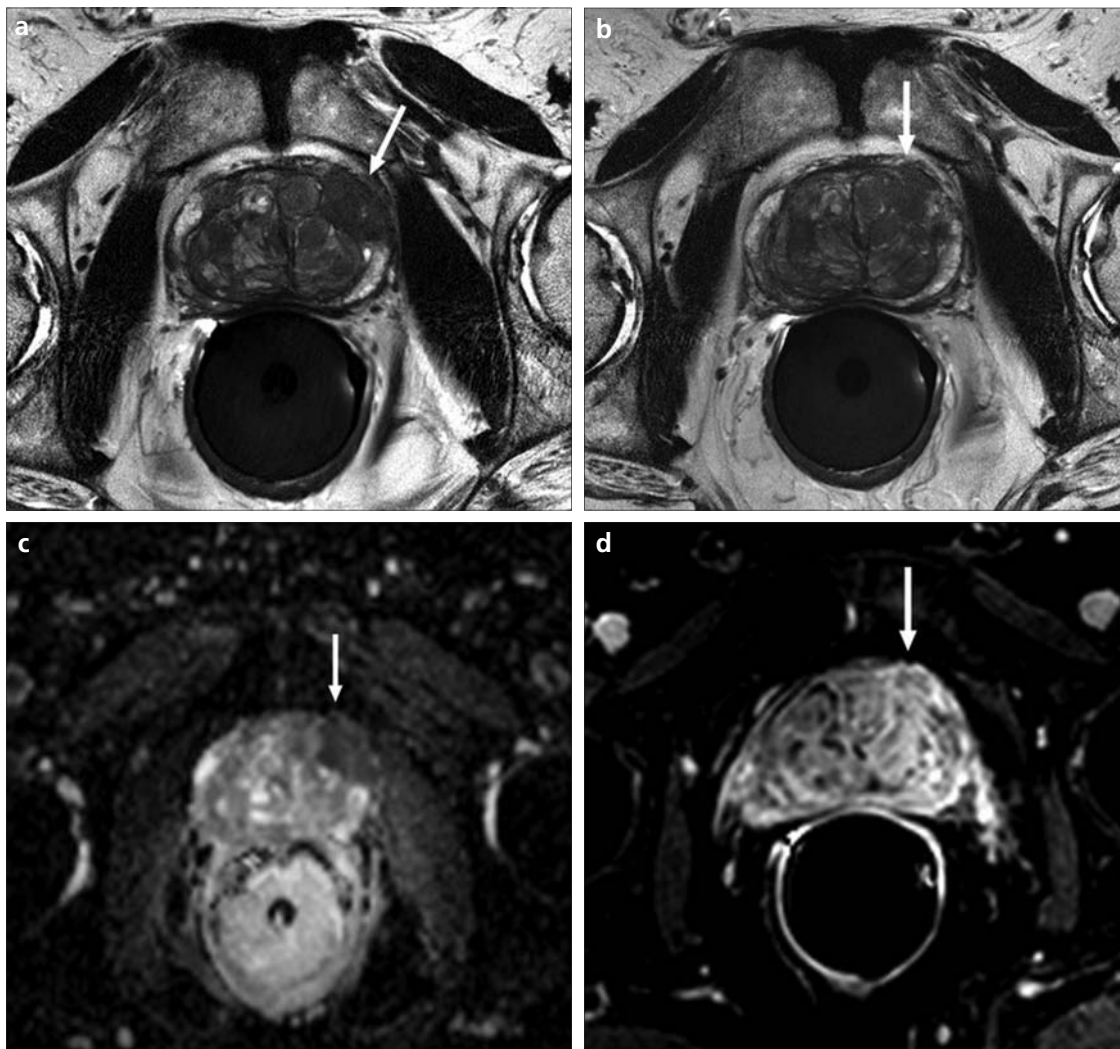
Figure 2. a–d. Anterior gland tumor with extracapsular extension in a 72-year-old man with history of adenocarcinoma of the left prostate gland (Gleason score on biopsy 4+4=8, PSA before surgery 20.2 ng/mL, TNM stage T3aN0M0 on both MRI and histopathology). An axial T2-weighted TSE MRI **(a)** of the midportion of the prostate shows a large, left anterior hypointense tumor in the prostate which is in broad contact with the prostatic capsule (*arrow*). An axial image from a slightly more superior level **(b)** reveals extracapsular extension of the tumor (*arrow*). An axial ADC map **(c)** shows restricted diffusion corresponding to the low signal intensity lesion on the T2-weighted images with capsular disruption (*arrow*). An axial postcontrast image **(d)** shows marked enhancement of the tumor with irregular capsular bulging.

DWI due to the dephasing of protons between the two diffusion gradients (33). When pathology causes an increase in tissue cellularity or cellular swelling, water motion becomes restricted and DWI shows high signal intensity in this area (34). Apparent diffusion coefficient (ADC) maps provide a quantitative analysis of DWI by measuring the degree of diffusion. When the diffusion of water molecules is restricted, the ADC value decreases. High b values (often 1000 s/mm^2) are commonly preferred in prostate MRI studies (35).

Diffusion tensor imaging (DTI) is a new emerging technique that is based on the calculation of anisotropic molecular diffusion of water molecules. DTI allows mapping of the microstructural fiber orientation of the tissue in three dimensions. Currently, DTI is more commonly used for investigating the normal prostatic structure and detecting prostate cancer. It has been reported that fiber tracking in the prostate may show the spread of cancer beyond the prostatic capsule (36).

Extracapsular extension with DWI

DWI and ADC maps have not been used to predict extracapsular extension in prostate cancer because of distortions, artifacts, and poor spatial resolution. Recent technical advancements, such as echo planar imaging with fat suppression, can provide increased signal-to-noise ratios and spatial resolutions and may be used for the evaluation of extracapsular extension (Figs. 1 and 2).

Seminal vesicle invasion with DWI

Restricted diffusion is also expected when the seminal vesicles are invaded by prostate cancer cells (Fig. 3), compared with normal seminal vesicles, which are mostly composed of seminal fluid with or without hemorrhage (37). Kim et al. (37) retrospectively evaluated the accuracy of combined T2-weighted MRI and DWI compared with T2-weighted MRI alone for predicting seminal vesicle invasion in patients with prostate cancer. This study was performed with a 3 T MRI, using a phased-array coil. The authors used ADC maps within the seminal vesicle without performing a quantitative analysis and reported that the use of T2-weighted MRI with DWI was more specific and accurate than that of T2-weighted MRI alone for the prediction of seminal vesicle invasion and noted that the addition of DWI to T2-weighted MRI showed significant improvement in diagnostic accuracy among less experienced readers. For the detection of seminal vesicle invasion in prostate cancer patients using 3 T MRI, T2-weighted images combined
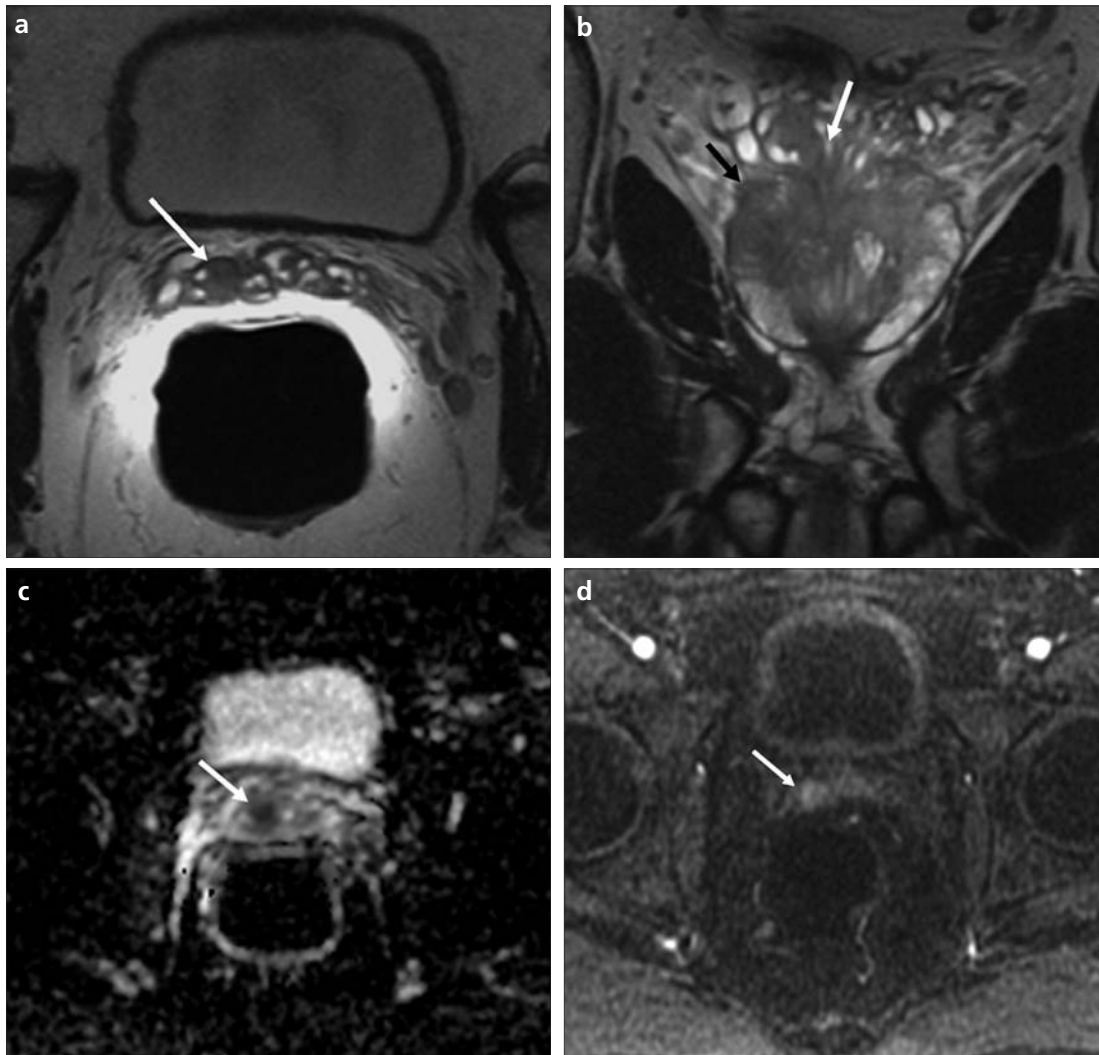
Figure 3. a–d. Seminal vesicle invasion of histopathologically confirmed stage T3b prostate cancer (Gleason score on biopsy 4+3=7, PSA before surgery 8.4 ng/mL, TNM stage T3bN0M0 on both MRI and histopathology) in a 61-year-old man. An axial T2-weighted TSE MRI (**a**) shows a focal low signal intensity lesion in the right seminal vesicle (*arrow*). A coronal T2-weighted TSE image (**b**) clearly shows the extension of the low signal intensity lesion from the prostate base, representing the cancer (*black arrow*), into the right seminal vesicle (*white arrow*). An axial ADC map (**c**) shows restricted diffusion corresponding to the low signal intensity lesion on the T2-weighted images (*arrow*). A subtraction image (**d**) shows early enhancement in the lesion invading the right seminal vesicle (*arrow*).

with DWI appear to be more accurate than T2-weighted imaging alone. Ren et al. (38) reported a higher accuracy rate in this setting in a study that compared the area under the receiver operating characteristic curve (AUC), which was 0.89 for the combination of T2-weighted MRI and DWI and 0.77 for T2-weighted MRI alone. Although some previously reported studies showed a significant overlap between ADC values for prostate cancer, benign prostate hyperplasia, prostatitis, and even normal tissue (39, 40), there are recent reports which have shown that DWI is valuable in detecting, localizing, and grading prostate cancer and the lowest ADC values may indicate the regions to be biopsied (41), and moreover DWI is more superior to DCE MRI in the detection of prostate cancer (42). Therefore, the routine use of DWI for seminal vesicle invasion requires validation.

Lymph node metastasis with DWI

DWI has also been evaluated in the analysis of pelvic lymph nodes. Eiber et al. (43) performed DWI of the pelvis at 1.5 T for investigating lymph node metastasis in patients with prostate cancer. The authors found a significant difference between the mean ADC value of malignant versus benign lymph nodes (43). However, there is still substantial overlap between ADC values of benign and malignant lymph nodes, which precludes the clinical use of DWI for lymph node characterization. Additionally, diffusion-weighted whole-body MRI with background body signal suppression has the potential to detect metastatic lymph nodes (44, 45).

DCE MRI

DCE MRI has emerged as a promising modality for prostate cancer imaging. The concept of DCE MRI is based on changes in the vascular characteristics of cancerous tissue compared with normal tissue. In cancerous tissue, angiogenesis (budding of new blood vessels), vasculogenesis (*de novo* formation of blood vessels), increased vascular permeability, and a larger interstitial space create a marked increase in the transfer rate of contrast material from the intravascular space to the extravascular/interstitial space. Time intensity curves and tracer kinetic models are used for extracting perfusion-related parameters from DCE MRI (Fig. 1) (46–50). Early, rapid, and strong enhancement with quick wash-out of contrast material is highly suggestive of prostate cancer in time-intensity curves (51, 52). Tracer kinetic models describe the microscopic distribution of contrast agent between the vascular and extravascular spaces over time. Various tracer kinetic models have been introduced by investigators. The
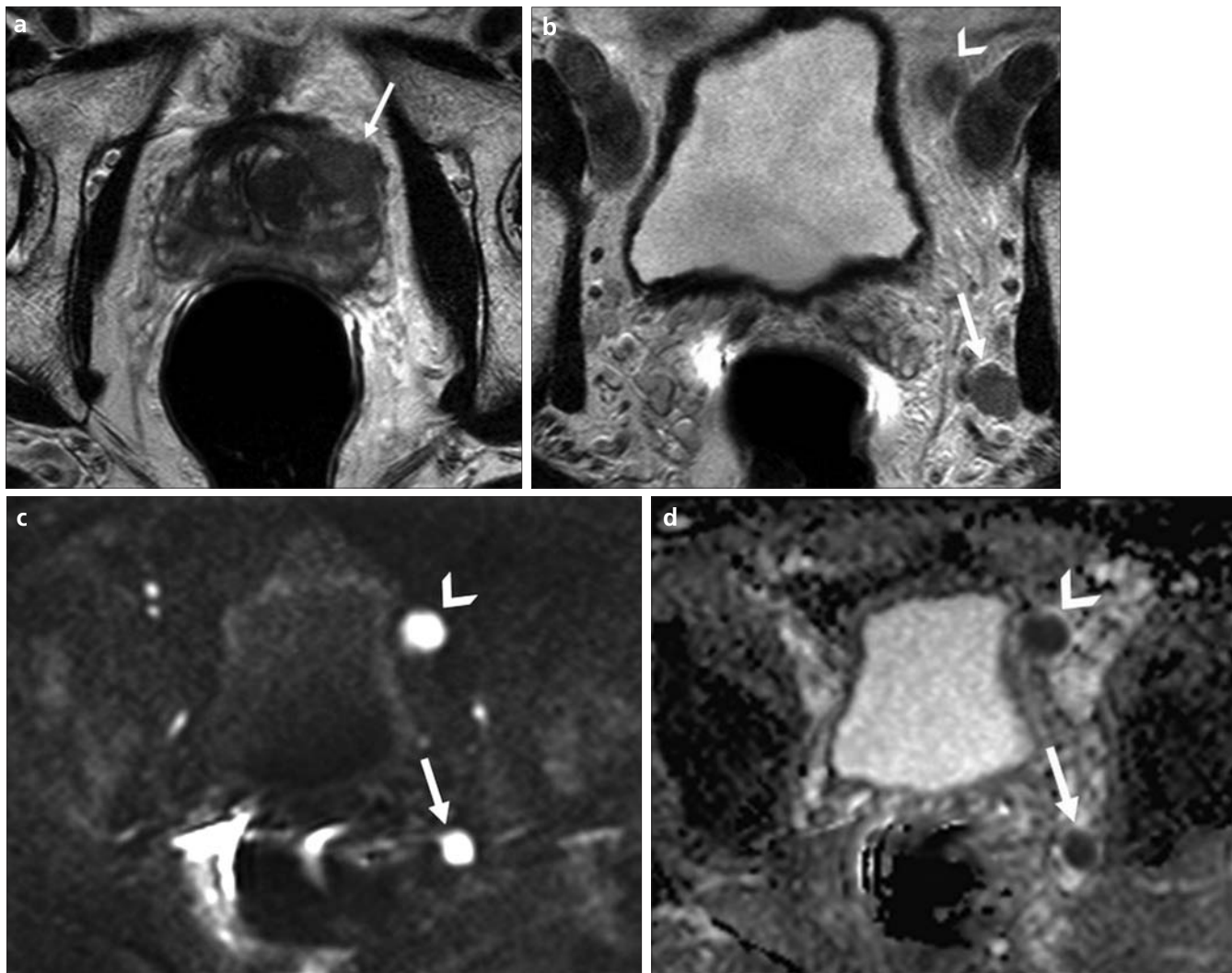
Figure 4. a–d. Metastatic lymph nodes in a 66-year-old man with history of adenocarcinoma of the left prostate gland (Gleason score on biopsy 4+3=7, PSA before surgery 12 ng/mL, TNM staging T3aN1 M0 on both MRI and histopathology). An axial T2-weighted TSE MRI (**a**) of the midportion of the prostate shows a hypointense tumor with extracapsular extension in the left prostate (*arrow*). An axial T2-weighted TSE image (**b**) shows left obturator *(arrow)* and left parailiac metastatic lymphadenopathy (*arrowhead*). DWI (**c**) and ADC maps (**d**) demonstrate restricted diffusion in the left-sided pelvic adenopathy (*arrows* and *arrowheads*).

two-compartment model is the most widely used pharmacokinetic model for DCE MRI analysis. In this model, K^{trans} is the influx constant between plasma and extravascular extracellular space (EES), v_e is the volume of EES per unit volume of tissue (leakage space), and k_{ep} is the efflux constant between the EES and the blood plasma. Limitations of this type of quantitative analysis include the large number of parameters that must be interpreted and a lack of consensus with regard to the optimal acquisition protocols and perfusion parameters for differentiating cancer from normal tissue. Additionally, these parameters may overlap considerably, decreasing the specificity of this technique for cancer detection (24, 47, 53).

Therefore, a standard MRI protocol for DCE MRI in prostate cancer staging as well as detection of prostate cancer, has not been completely established. Further comprehensive studies of this technique are needed, including fast imaging sequences, minimal artifacts, and high contrast resolution. To increase the accuracy of imaging, DCE MRI should be performed with fast temporal resolution, (<3 s) high spatial resolution and long acquisition times (54).

Extracapsular extension with DCE MRI

Previous DCE MRI studies obtained high temporal resolution at the expense of spatial resolution. These techniques used thick sections and had

lower accuracy rates for prostate cancer staging (24, 47). Bloch et al. (54) reported that addition of high spatial-resolution DCE MRI has improved the accuracy of T2-weighted MRI compared with T2-weighted MRI alone in the assessment of extracapsular extension (AUC 86% vs. 96%, respectively). In their study, color-coded schemes were obtained with a model that incorporated three time points from the DCE MRI. These images were analyzed for the presence of bright red extracapsular pixel clusters larger than 3 mm in diameter, which are considered to be suspicious for extracapsular extension (54). Fütterer et al. (55) fused parametric maps of DCE MRI with T2-weighted images in an attempt to differentiate

stage T2 from stage T3 prostate cancer. The authors used the following DCE MRI parameters to evaluate the presence of extracapsular extension in prostate cancer: presence of high peak enhancement, asymmetric high peak enhancement, wash-out, and shorter onset time or increased time-to-peak. They reported that the addition of DCE MRI can significantly improve the interpretation of less experienced readers compared with T2-weighted MRI alone (AUC 66%, 82%, respectively), but that it made no additional contribution to experienced readers' staging performance (55).

Seminal vesicle invasion with DCE MRI

The combination of peak enhancement with the presence of contrast material wash-out is highly suggestive of prostate cancer, both for peripheral and central cancers (47, 51). Ogura et al. (56) interpreted early enhancement in the seminal vesicles on dynamic T1-weighted images as seminal vesicle invasion and reported that this finding has accuracy rates as high as 97% for seminal vesicle invasion. Fütterer et al. (55) found that the addition of contrast-enhanced MRI only benefited less experienced readers in terms of determining whether seminal vesicle invasion and extracapsular extension were present.

Lymph node metastasis with DCE MRI

To our knowledge, no studies have evaluated the ability of DCE MRI to diagnose lymph node metastasis from prostate cancer. Another novel technique, MR lymphography, has been introduced recently. MR lymphography uses intravenously administered ferumoxtran-10, which belongs to a class of nanoparticle-based contrast agents that are referred to as ultrasmall superparamagnetic iron oxide. Harisinghani et al. (57) reported high sensitivity (100%) and specificity (95.7%) values in a study investigating lymph node metastasis of the prostate cancer with this technique. A clear advantage of MR lymphography is that it is able to detect small metastatic lymph nodes. Although these agents were recently pulled from the market and are not currently available, clinical trials are continuing with a derivative of ferumoxtran-10, ferumoxytol, for the detection of lymph node involvement in prostate cancer.

MRS

MRS is based on the chemical shift resulting from the shield formed by the electron cloud surrounding hydrogen nuclei in molecules (58). MRS identifies metabolites of interest in prostate tissue by locating the peaks of chemical compounds. In prostate cancer, increases in the choline and creatine peaks and a decrease in the citrate peak are expected findings (Fig. 5). MRS requires a very homogeneous magnetic field (shimming). Advanced operating skills are also needed for post-processing of the prostatic spectra to achieve high-quality data, so the process has a relatively long post-processing time. Post-biopsy hemorrhage lowers the sensitivity of MRS by degrading the MR spectra (59).

MRS has a high specificity for prostate cancer detection, but it has a low sensitivity because of partial volume effects and strong signals from the surrounding tissue, especially the seminal vesicles, stromal benign prostatic hyperplasia and prostatitis (60).

Local staging with MRS

Studies that investigated MRS as a method of detecting extracapsular extension in patients with prostate cancer are somewhat controversial. It has been reported that using MRS with conventional MRI may improve overall staging by identifying foci of extracapsular disease (10). Yu et al. (61) reported that the addition of three-dimensional (3D) MRS imaging to MRI improved the diagnostic accuracy for extracapsular extension only among less experienced readers. These authors used the location and number of abnormal MRS voxels as the primary MRS imaging data for the evaluation of extracapsular extension (61). In their study, patients with the least extensive tumors on 3D MRS (<1 cancer voxel per section) were found to have only a 6% risk for extracapsular extension, whereas patients with the most extensive tumors (>4 cancer voxels per section) had an 80% risk of extracapsular extension (61). The authors therefore claimed that 3D MRS has potential as a predictor of extracapsular extension (61). Because the resolution of MRS is lower than that of conventional MRI, MRS may not depict small foci of extracapsular spread. Wetter et al. (62) showed that there is no significant improvement in detecting extracapsular extension in patients with prostate cancer when using MRI vs. MRS. MRS is therefore not recommended for use in the routine staging of prostate carcinoma (62).

MRS does not play a role in the assessment of the probability of seminal vesicle invasion. No comprehensive study in the literature has used MRS to detect lymph node involvement in prostate cancer. However, Heijmink et al. (63) reported high choline levels in an enlarged metastatic lymph node in a patient with recurrent prostate cancer. They claimed that it was possible to use MRS with a 3 T MRI to quantify the total amount of choline-containing compounds in lymph node metastases located deep inside the body (63).

Conclusion

Accurate local staging of prostate cancer is essential for the management of this disease. T2-weighted scans are still the main MRI sequence for local staging in prostate cancer. DWI, DCE MRI, and MRS are available but evolving techniques and can be considered as a part of a multi-modality MRI protocol for imaging of the prostate gland. To interpret these studies accurately, radiologists should be aware of the advantages, limitations, and technical background of these functional techniques. There is still a need for multi-institutional trials to standardize functional MRI techniques and interpretation criteria.

Conflict of interest disclosure

The authors declared no conflicts of interest.

References

1. Edge SB, Byrd DR, Compton CC, Fritz AG, Greene FL, Trotti A. AJCC cancer staging manual. 7th ed. New York, NY: Springer, 2010; 457–468.
2. Hull GW, Rabbani F, Abbas F, Wheeler TM, Kattan MW, Scardino PT. Cancer control with radical prostatectomy alone in 1,000 consecutive patients. J Urol 2002; 167:528–534.
3. Ohori M, Kattan MW, Koh H, et al. Predicting the presence and side of extracapsular extension: a nomogram for staging prostate cancer. J Urol 2004; 171:1844–1849.
4. Epstein JI, Partin AW, Potter SR, Walsh PC. Adenocarcinoma of the prostate invading the seminal vesicle: prognostic stratification based on pathologic parameters. Urology 2000; 56:283–288.
5. Cagiannos I, Karakiewicz P, Eastham JA, et al. A preoperative nomogram identifying decreased risk of positive pelvic lymph nodes in patients with prostate cancer. J Urol 2003; 170:1798–1803.

6. Gervasi LA, Mata J, Easley JD, Wilbanks JH, et al. Prognostic significance of lymph nodal metastases in prostate cancer. J Urol 1989; 142:332–336.

7. Partin AW, Kattan MW, Subong EN, et al. Combination of prostate-specific antigen, clinical stage, and Gleason score to predict pathological stage of localized prostate cancer. A multi-institutional update. JAMA 1997; 277:1445–1451.

8. Partin AW, Mangold LA, Lamm DM, Walsh PC, Epstein JI, Pearson JD. Contemporary update of prostate cancer staging nomograms (Partin tables) for the new millennium. Urology 2001; 58:843–848.

9. Koh H, Kattan MW, Scardino PT, et al. A nomogram to predict seminal vesicle invasion by the extent and location of cancer in systematic biopsy results. J Urol 2003; 170:1203–1208.

10. Wang L, Hricak H, Kattan MW, Chen HN, Scardino PT, Kuroiwa K. Prediction of organ-confined prostate cancer: incremental value of MR imaging and MR spectroscopic imaging to staging nomograms. Radiology 2006; 238:597–603.

11. Fütterer JJ. MR imaging in local staging of prostate cancer. Eur J Radiol 2007; 63:328–334.

12. Engelbrecht MR, Jager GJ, Laheij RJ, Verbeek AL, van Lier HJ, Barentsz JO. Local staging of prostate cancer using magnetic resonance imaging: a meta-analysis. Eur Radiol 2002; 12:2294–2302.

13. Perrotti M, Kaufman RP Jr, Jennings TA, et al. Endo-rectal coil magnetic resonance imaging in clinically localized prostate cancer: is it accurate? J Urol 1996; 156:106–109.

14. Hricak H, White S, Vigneron D, et al. Carcinoma of the prostate gland: MR imaging with pelvic phased-array coils versus integrated endorectal-pelvic phased-array coils. Radiology 1994; 193:703–709.

15. Choi H, Ma J. Use of perfluorocarbon compound in the endorectal coil to improve MR spectroscopy of the prostate. AJR Am J Roentgenol 2008; 190:1055–1059.

16. Rosen Y, Bloch BN, Lenkinski RE, Greenman RL, Marquis RP, Rofsky NM. 3T MR of the prostate: reducing susceptibility gradients by inflating the endorectal coil with a barium sulfate suspension. Magn Reson Med 2007; 57:898–904.

17. Heijmink SW, Fütterer JJ, Hambrock T, et al. Prostate cancer: body-array versus endorectal coil MR imaging at 3 T—comparison of image quality, localization, and staging performance. Radiology 2007; 244:184–195.

18. Dickinson L, Ahmed HU, Allen C, et al. Magnetic resonance imaging for the detection, localisation, and characterisation of prostate cancer: recommendations from a European consensus meeting. Eur Urol 2011; 59:477–494.

19. Wang L, Zhang J, Schwartz LH, et al. Incremental value of multiplanar cross-referencing for prostate cancer staging with endorectal MRI. AJR Am J Roentgenol 2007; 188:99–104.

20. Sala E, Akin O, Moskowitz CS, et al. Endorectal MR imaging in the evaluation of seminal vesicle invasion: diagnostic accuracy and multivariate feature analysis. Radiology 2006; 238:929–937.

21. Schiebler ML, Yankaskas BC, Tempany C, et al. MR imaging in adenocarcinoma of the prostate: interobserver variation and efficacy for determining stage C disease. AJR Am J Roentgenol 1992; 158:559–562.

22. Biondetti PR, Lee JK, Ling D, Catalona WJ. Clinical stage B prostate carcinoma: staging with MR imaging. Radiology 1987; 162:325–329.

23. Rorvik J, Halvorsen OJ, Albrektsen G, Ersland L, Daehlin L, Haukaas S. MRI with an endorectal coil for staging of clinically localized prostate cancer prior to radical prostatectomy. Eur Radiol 1999; 9:29–34.

24. Padhani AR, Gapinski CJ, Macvicar DA, et al. Dynamic contrast enhanced MRI of prostate cancer: correlation with morphology and tumour stage, histological grade and PSA. Clin Radiol 2000; 55:99–109.

25. Yu KK, Hricak H, Alagappan R, Chernoff DM, Bacchetti P, Zaloudek CJ. Detection of extracapsular extension of prostate carcinoma with endorectal and phased-array coil MR imaging: multivariate feature analysis. Radiology 1997; 202:697–702.

26. Wang L, Mullerad M, Chen HN, et al. Prostate cancer: incremental value of endorectal MR imaging findings for prediction of extracapsular extension. Radiology 2004; 232:133–139.

27. Tempany CM, Rahmouni AD, Epstein JI, Walsh PC, Zerhouni EA. Invasion of the neurovascular bundle by prostate cancer: evaluation with MR imaging. Radiology 1991; 181:107–112.

28. Jung DC, Lee HJ, Kim SH, Choe GY, Lee SE. Preoperative MR imaging in the evaluation of seminal vesicle invasion in prostate cancer: pattern analysis of seminal vesicle lesions. J Magn Reson Imaging 2008; 28:144–150.

29. Schnall MD, Imai Y, Tomaszewski J, Pollack HM, Lenkinski RE, Kressel HY. Prostate cancer: local staging with endorectal surface coil. MR imaging. Radiology 1991; 178:797–802.

30. Wang L, Hricak H, Kattan MW, et al. Combined endorectal and phased-array MRI in the prediction of pelvic lymph node metastasis in prostate cancer. AJR Am J Roentgenol 2006; 186:743–748.

31. Jager GJ, Barentsz JO, Oosterhof GO, Witjes JA, Ruijs SJ. Pelvic adenopathy in prostatic and urinary bladder carcinoma: MR imaging with a three-dimensional TI-weighted magnetization-prepared-rapid gradient-echo sequence. AJR Am J Roentgenol 1996; 167:1503–1507.

32. Borley N, Fabrin K, Sriprasad S, et al. Laparoscopic pelvic lymph node dissection allows significantly more accurate staging in "high-risk" prostate cancer compared to MRI or CT. Scand J Urol Nephrol 2003; 37:382–386.

33. Le Bihan D. Diffusion/perfusion MR imaging of the brain: from structure to function. Radiology 1990; 177:328–329.

34. Gauvain KM, McKinstry RC, Mukherjee P, et al. Evaluating pediatric brain tumor cellularity with diffusion-tensor imaging. AJR Am J Roentgenol 2001; 177:449–454.

35. Rosenkrantz AB, Mannelli L, Kong X, et al. Prostate cancer: utility of fusion of T2-weighted and high b-value diffusion-weighted images for peripheral zone tumor detection and localization. J Magn Reson Imaging 2011; 34:95–100.

36. Manenti G, Carlani M, Mancino S, et al. Diffusion tensor magnetic resonance imaging of prostate cancer. Invest Radiol 2007; 42:412–419.

37. Kim CK, Choi D, Park BK, Kwon GY, Lim HK. Diffusion-weighted MR imaging for the evaluation of seminal vesicle invasion in prostate cancer: initial results. J Magn Reson Imaging 2008; 28:963–969.

38. Ren J, Huan Y, Wang H, et al. Seminal vesicle invasion in prostate cancer: prediction with combined T2-weighted and diffusion-weighted MR imaging. Eur Radiol 2009; 19:2481–2486.

39. Lim HK, Kim JK, Kim KA, Cho KS. Prostate cancer: apparent diffusion coefficient map with T2-weighted images for detection-a multireader study. Radiology 2009; 250:145–151.

40. Kim JH, Kim JK, Park BW, Kim N, Cho KS. Apparent diffusion coefficient: prostate cancer versus noncancerous tissue according to anatomical region. J Magn Reson Imaging 2008; 28:1173–1179.

41. Yağci AB, Ozari N, Aybek Z, Düzcan E. The value of diffusion-weighted MRI for prostate cancer detection and localization. Diagn Interv Radiol 2011; 17:130–134.

42. Iwazawa J, Mitani T, Sassa S, Ohue S. Prostate cancer detection with MRI: is dynamic contrast-enhanced imaging necessary in addition to diffusion-weighted imaging? Diagn Interv Radiol 2011; 17:243–248.

43. Eiber M, Beer AJ, Holzapfel K, et al. Preliminary results for characterization of pelvic lymph nodes in patients with prostate cancer by diffusion-weighted MR-imaging. Invest Radiol 2010; 45:15–23.

44. Kwee TC, Takahara T, Ochiai R, Nievelstein RA, Luijten PR. Diffusion-weighted whole-body imaging with background body signal suppression (DWIBS): features and potential applications in oncology. Eur Radiol 2008; 18:1937–1952.

45. Eiber M, Holzapfel K, Ganter C, et al. Whole-body MRI including diffusion-weighted imaging (DWI) for patients with recurring prostate cancer: technical feasibility and assessment of lesion conspicuity in DWI. J Magn Reson Imaging 2011; 33:1160–1170.

46. Moate PJ, Dougherty L, Schnall MD, Landis RJ, Boston RC. A modified logistic model to describe gadolinium kinetics in breast tumors. Magn Reson Imaging 2004; 22:467–473.

47. Engelbrecht MR, Huisman HJ, Laheij RJ, et al. Discrimination of prostate cancer from normal peripheral zone and central gland tissue by using dynamic contrast-enhanced MR imaging. Radiology 2003; 229:248–254.

48. Kayhan A, Fan X, Oto A. Dynamic contrast-enhanced magnetic resonance imaging in prostate cancer. Top Magn Reson Imaging 2009; 20:105–112.

49. Tofts PS, Brix G, Buckley DL, et al. Estimating kinetic parameters from dynamic contrast-enhanced T(1)-weighted MRI of a diffusible tracer: standardized quantities and symbols. J Magn Reson Imaging 1999; 10:223–232.

50. Ocak I, Bernardo M, Metzger G, et al. Dynamic contrast-enhanced MRI of prostate cancer at 3 T: a study of pharmacokinetic parameters. AJR Am J Roentgenol 2007; 189:849.

51. Alonzi R, Padhani AR, Allen C. Dynamic contrast enhanced MRI in prostate cancer. Eur J Radiol 2007; 63:335–350.

52. Sciarra A, Panebianco V, Ciccariello M, et al. Magnetic resonance spectroscopic imaging (1H-MRSI) and dynamic contrast-enhanced magnetic resonance (DCE-MRI): pattern changes from inflammation to prostate cancer. Cancer Invest 2010; 28:424–432.

53. Kim JK, Hong SS, Choi YJ, et al. Wash-in rate on the basis of dynamic contrast-enhanced MRI: usefulness for prostate cancer detection and localization. J Magn Reson Imaging 2005; 22:639–646.

54. Bloch BN, Furman-Haran E, Helbich TH, et al. Prostate cancer: accurate determination of extracapsular extension with high-spatial-resolution dynamic contrast-enhanced and T2-weighted MR imaging—initial results. Radiology 2007; 245:176–185.

55. Fütterer JJ, Engelbrecht MR, Huisman HJ, et al. Staging prostate cancer with dynamic contrast-enhanced endorectal MR imaging prior to radical prostatectomy: experienced versus less experienced readers. Radiology 2005; 237:541–549.

56. Ogura K, Maekawa S, Okubo K, et al. Dynamic endorectal magnetic resonance imaging for local staging and detection of neurovascular bundle involvement of prostate cancer: correlation with histopathologic results. Urology 2001; 57:721–726.

57. Harisinghani MG, Barentsz J, Hahn PF, et al. Noninvasive detection of clinically occult lymph-node metastases in prostate cancer. N Engl J Med 2003; 348:2491–2499.

58. Bonekamp D, Jacobs MA, El-Khouli R, Stoianovici D, Macura KJ. Advancements in MR imaging of the prostate: from diagnosis to interventions. Radiographics 2011; 31:677–703.

59. Qayyum A, Coakley FV, Lu Y, et al. Organ-confined prostate cancer: effect of prior transrectal biopsy on endorectal MRI and MR spectroscopic imaging. AJR Am J Roentgenol 2004; 183:1079–1083.

60. Prando A, Billis A. Focal prostatic atrophy: mimicry of prostatic cancer on TRUS and 3D-MRSI studies. Abdom Imaging 2009; 34:271–275.

61. Yu KK, Scheidler J, Hricak H, et al. Prostate cancer: prediction of extracapsular extension with endorectal MR imaging and three-dimensional proton MR spectroscopic imaging. Radiology 1999; 213:481–488.

62. Wetter A, Engl TA, Nadjmabadi D, et al. Combined MRI and MR spectroscopy of the prostate before radical prostatectomy. AJR Am J Roentgenol 2006; 187:724–730.

63. Heijmink SW, Scheenen TW, Fütterer JJ, et al. Prostate and lymph node proton magnetic resonance (MR) spectroscopic imaging with external array coils at 3 T to detect recurrent prostate cancer after radiation therapy. Invest Radiol 2007; 42:420–427.